

SUPPORTING INFORMATION

Isoselective 4-Methylpentene Polymerization by Pyridylamido Hafnium Catalysts

Lingzhi Wang,^a Donghui Li,^a He Ren,^b Yuru Wang,^b Wei Wu,^b Yuxin Gao,^b Xiong
Wang,^c and Haiyang Gao^{*a}

^a School of Materials Science and Engineering, PCFM Lab, GD HPPC Lab, Sun Yat-sen University, Guangzhou 510275, China.

^b Daqing Chemical Engineering Research Center, Petrochemical Research Institute, CNPC, Daqing 163714, China.

^c Lanzhou Petrochemical Research Center, Petrochemical Research Institute, PetroChina, Lanzhou 730060, China.

* Corresponding author. Fax: +86-20-84114033. Tel.: +86-20-84113250. E-mail: Gao H.: gaohy@mail.sysu.edu.cn

Content

1. Characterization of Pyridylamido Hafnium Complexes.....	2
2. GPC traces of polymers	4
3. DSC curves of polymers	5
4. NMR characterizations of polymers	7
5. XRD patterns of polymers	8

1. Characterization of Pyridylamido Hafnium Complexes

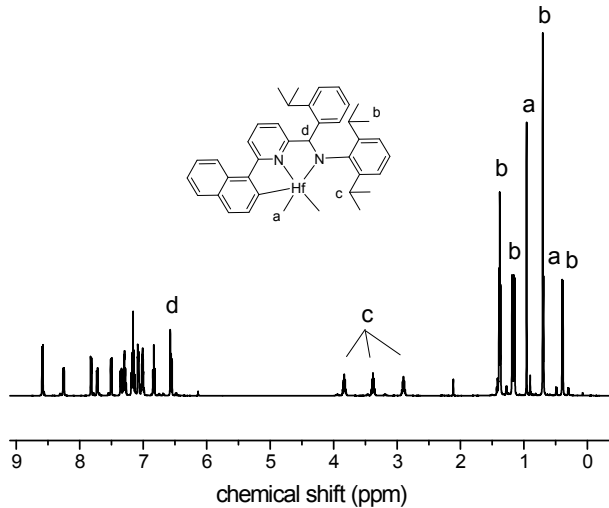


Figure S1. ¹H NMR spectrum of complex **1** in C₆D₆.

¹H NMR (C₆D₆, 400 MHz): δ (ppm) 8.58 (d, 1H, Nap-*H*), 8.25 (d, 1H, Nap-*H*), 7.81 (d, 1H, Nap-*H*), 7.72 (d, 1H, Nap-*H*), 7.50 (d, 1H, Py-*H*), 7.36-7.00 (m, 9H, Ar-*H*), 6.83 (d, 1H, Py-*H*), 6.57 (s, 1H, NCH), 6.55 (d, 1H, Py-*H*), 3.83 (sept, 1H, CH(CH₃)₂), 3.34 (sept, 1H, CH(CH₃)₂), 2.90 (sept, 1H, CH(CH₃)₂), 1.38 (d, 3H, CH(CH₃)₂), 1.36 (d, 3H, CH(CH₃)₂), 1.19 (d, 3H, CH(CH₃)₂), 1.15 (d, 3H, CH(CH₃)₂), 0.96 (s, 3H, Hf-CH₃), 0.71 (d, 3H, CH(CH₃)₂), 0.69 (s, 3H, Hf-CH₃), 0.39 (d, 3H, CH(CH₃)₂).

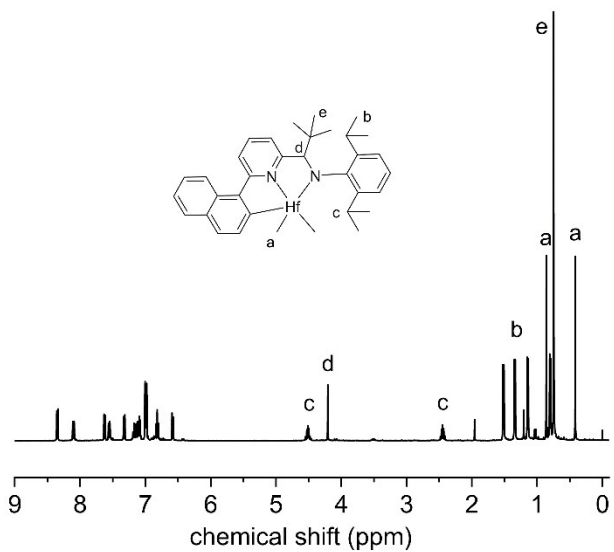


Figure S2. ^1H NMR spectrum complex **2** in C_6D_6 .

^1H NMR (C_6D_6 , 400 MHz): δ (ppm) 8.53 (d, 1H, Nap-*H*), 8.28 (d, 1H, Nap-*H*), 7.80 (d, 1H, Nap-*H*), 7.73 (d, 1H, Nap-*H*), 7.50 (d, 1H, Py-*H*), 7.36-7.25 (m, 4H, Ar-*H*), 7.03-6.97 (m, 2H, Ar-*H*), 6.76 (d, 1H, Py-*H*), 4.68 (sept, 1H, $\text{CH}(\text{CH}_3)_2$), 4.37 (s, 1H, NCH), 2.62 (sept, 1H, $\text{CH}(\text{CH}_3)_2$), 1.78 (d, 3H, $\text{CH}(\text{CH}_3)_2$), 1.61 (d, 3H, $\text{CH}(\text{CH}_3)_2$), 1.41 (d, 3H, $\text{CH}(\text{CH}_3)_2$), 1.12 (s, 3H, Hf- CH_3), 1.08 (d, 3H, $\text{CH}(\text{CH}_3)_2$), 1.00 (s, 9H, $\text{C}(\text{CH}_3)_3$), 0.67 (s, 3H, Hf- CH_3).

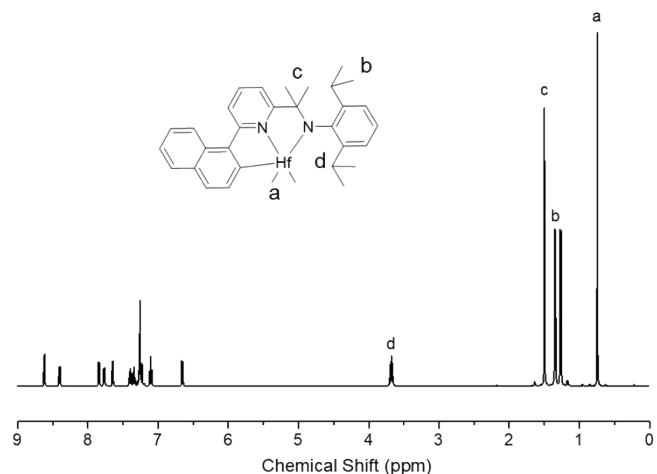


Figure S3. ^1H NMR spectrum of complex **3** in C_6D_6 .

$^1\text{HNMR}$ (C_6D_6 , 400 MHz): δ (ppm) 8.56 (d, 1H, Ar-*H*), 8.35 (d, 1H, Ar-*H*), 7.78 (d, 1H, Ar-*H*), 7.70 (dd, 1.5 Hz, 1H, Ar-*H*), 7.57 (d, 1H, Ar-*H*), 7.35-7.18 (m, 4H, Ar-*H*), 7.02

(t, 1H, Ar-H), 6.57 (d, 1H, Ar-H), 3.61 (sept, 2H, CH(CH₃)₂), 1.43 (s, 6H, (CH₃)₂C), 1.28 (d, 6H, CH(CH₃)₂), 1.20 (d, 6H, CH(CH₃)₂), 0.69 (s, 6H, Hf-CH₃).

2. GPC traces of polymers

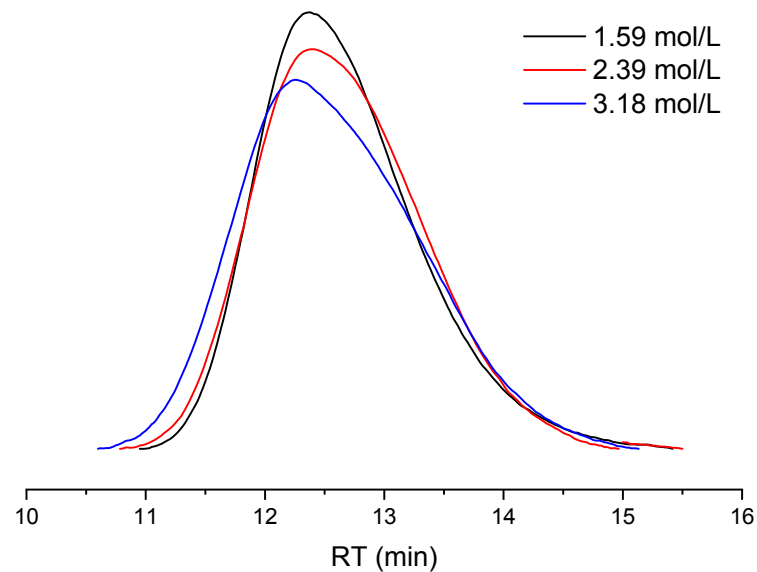


Figure S4. GPC traces of PMPs produced by **1** at different monomer concentrations.

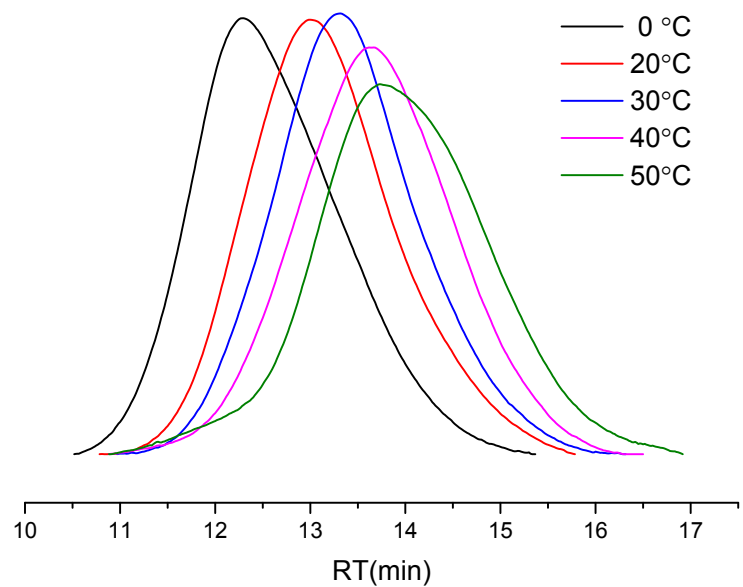


Figure S5. GPC traces of PMPs produced by **2** at different temperatures.

3. DSC curves of polymers

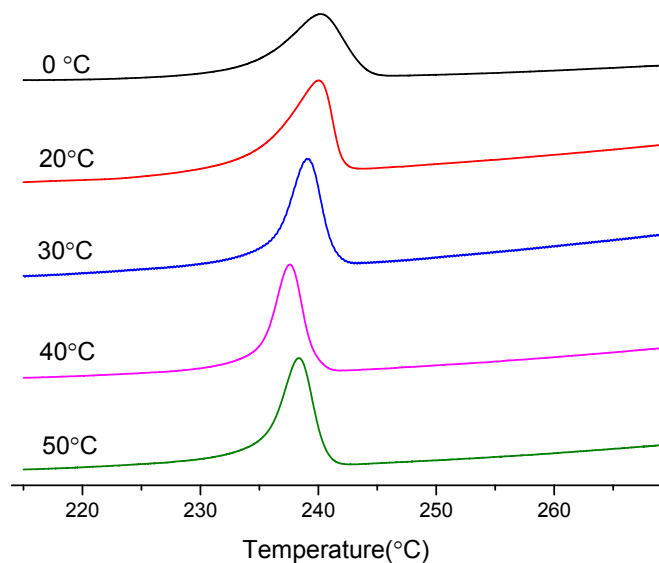


Figure S6. DSC curves of PMPs produced by **1** at different temperatures.

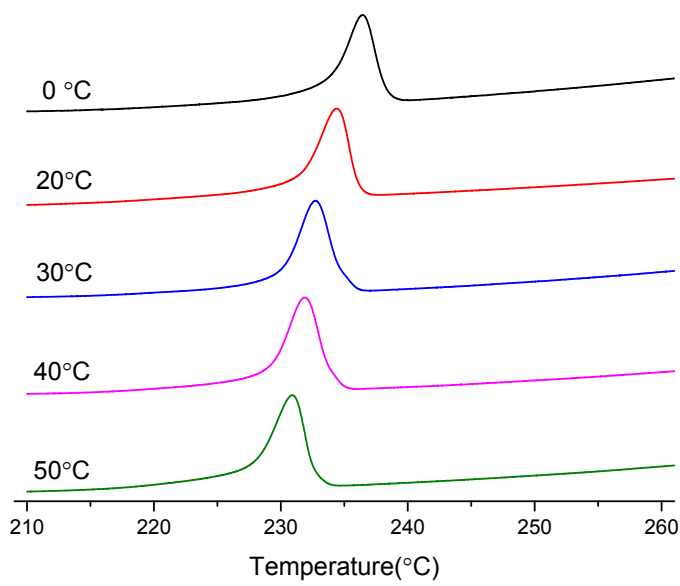


Figure S7. DSC curves of PMPs produced by **2** at different temperatures.

4. NMR characterization of polymers

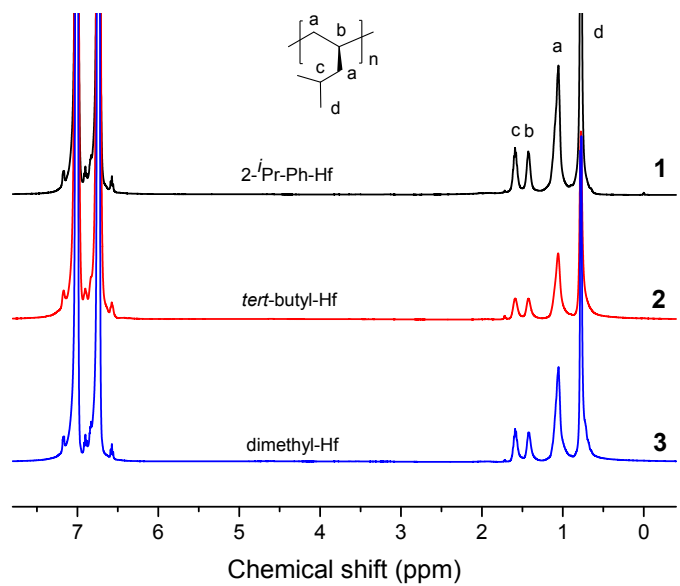


Figure S8. ¹H NMR spectra of PMPs produced by **1**, **2**, and **3** at 40 °C.

5. XRD patterns of polymers

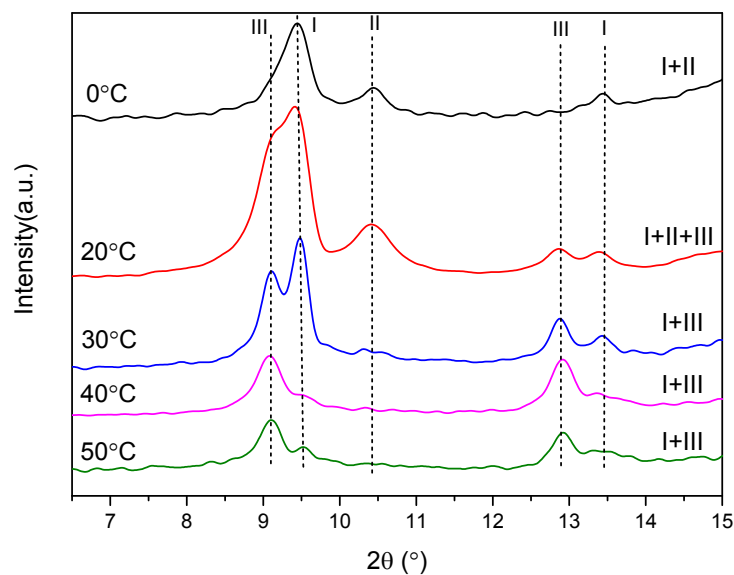


Figure S9. Magnified X-ray powder diffraction patterns of PMPs produced by **1** at different temperatures.

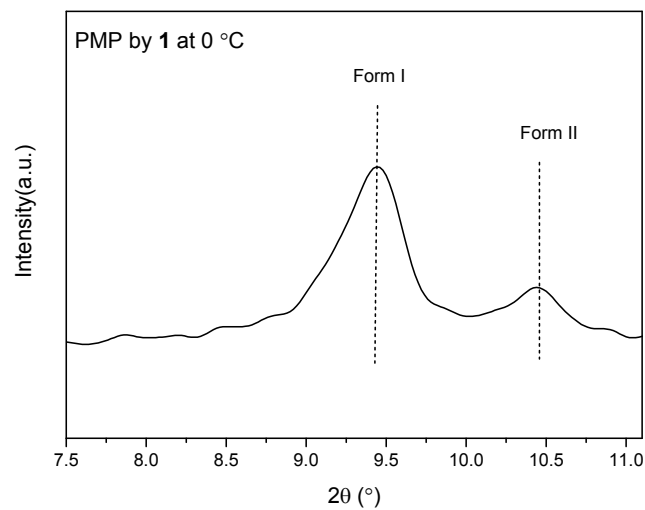


Figure S10. Peak separation of the X-ray diffraction patterns by **1** at 0 °C.

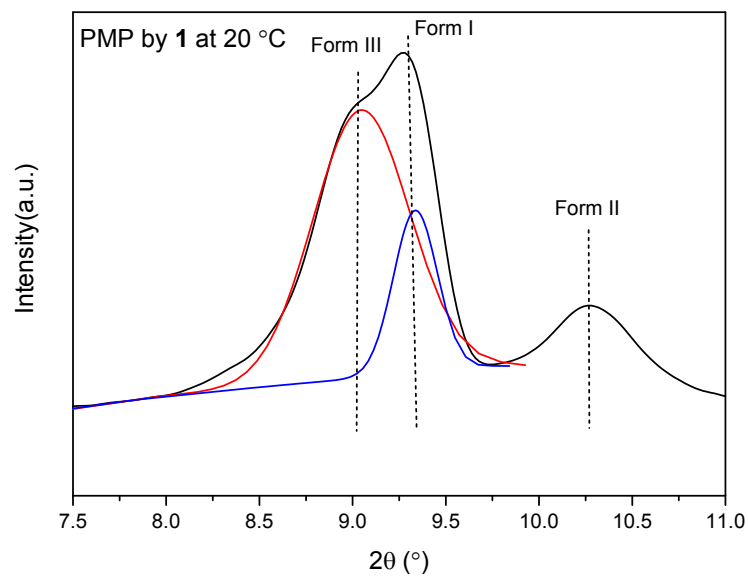


Figure S11. Peak separation of the X-ray diffraction patterns by **1** at 20 °C.

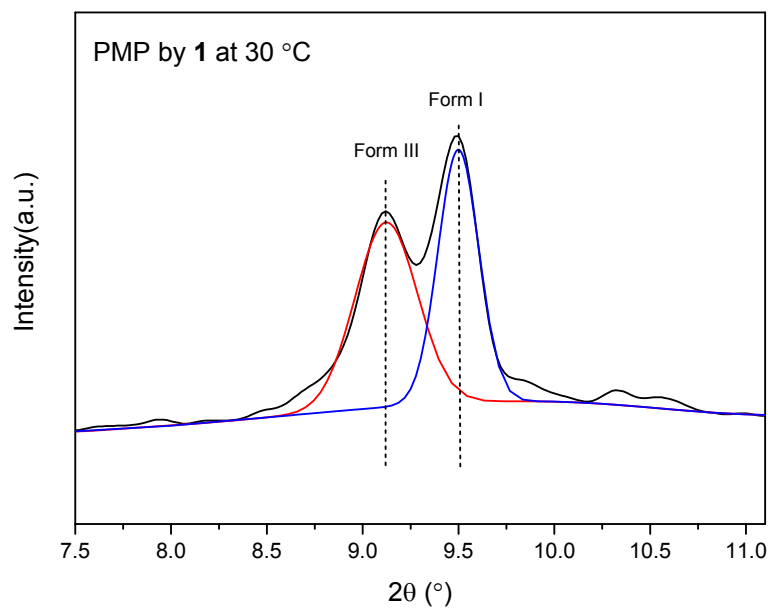


Figure S12. Peak separation of the X-ray diffraction patterns by **1** at 30 °C.

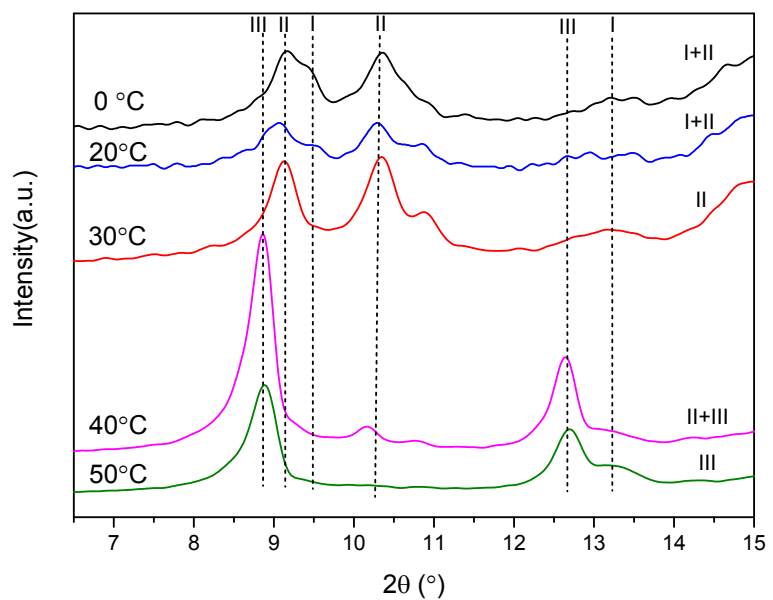


Figure S13. Magnified X-ray powder diffraction patterns of PMPs produced by **2** at different temperatures.

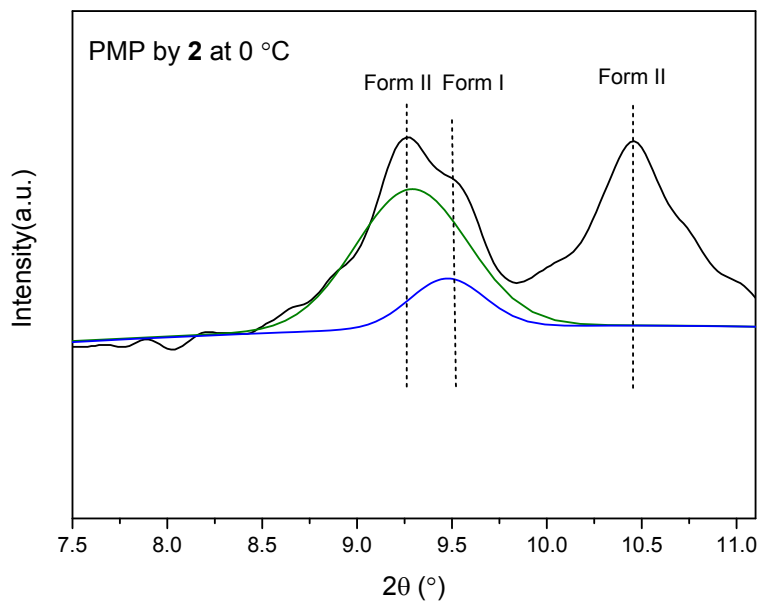


Figure S14. Peak separation of the X-ray diffraction patterns by **2** at 0 °C.

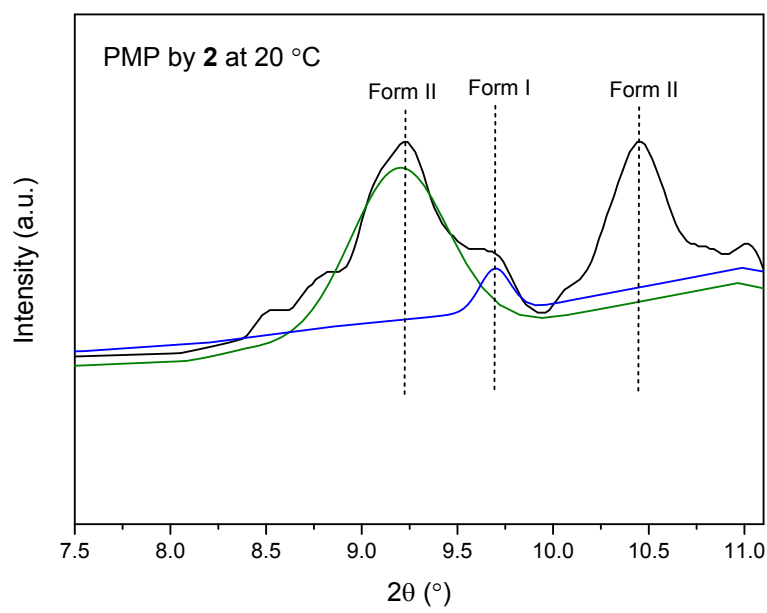


Figure S15. Peak separation of the X-ray diffraction patterns by **2** at 20 °C.

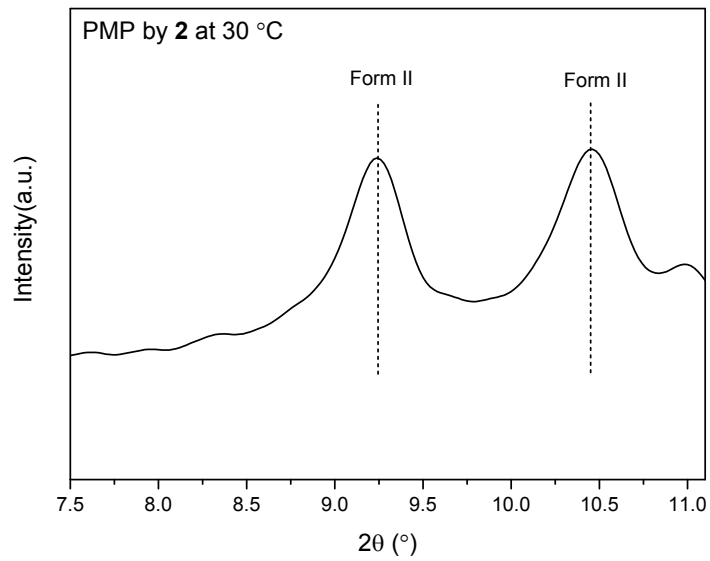


Figure S16. Peak separation of the X-ray diffraction patterns by **2** at 30 °C.

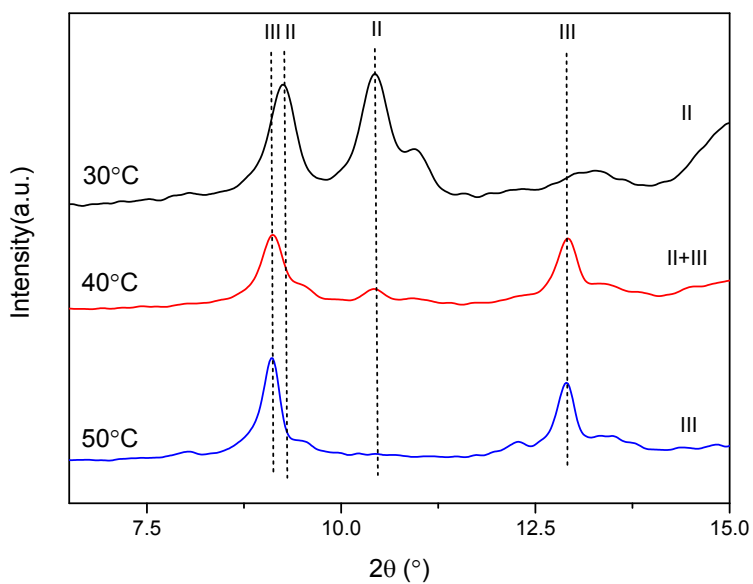


Figure S17. X-ray powder diffraction patterns of PMPs produced by **3** at different temperatures.

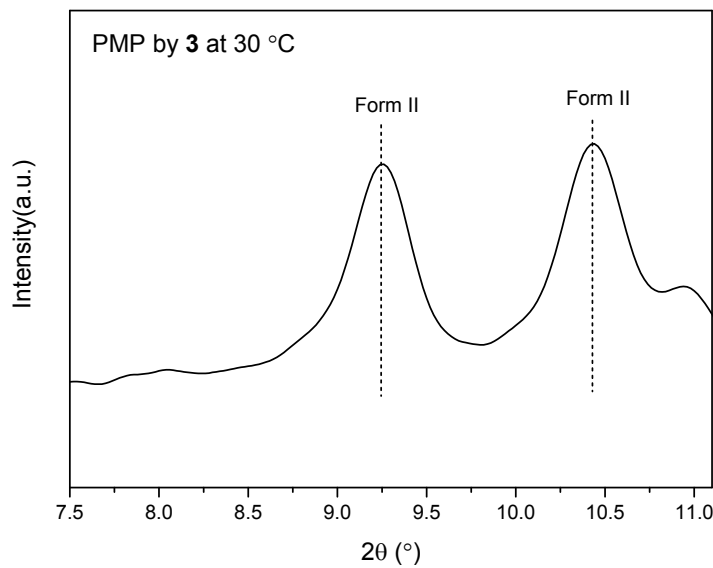


Figure S18. Peak separation of the X-ray diffraction patterns by **3** at 30 °C.

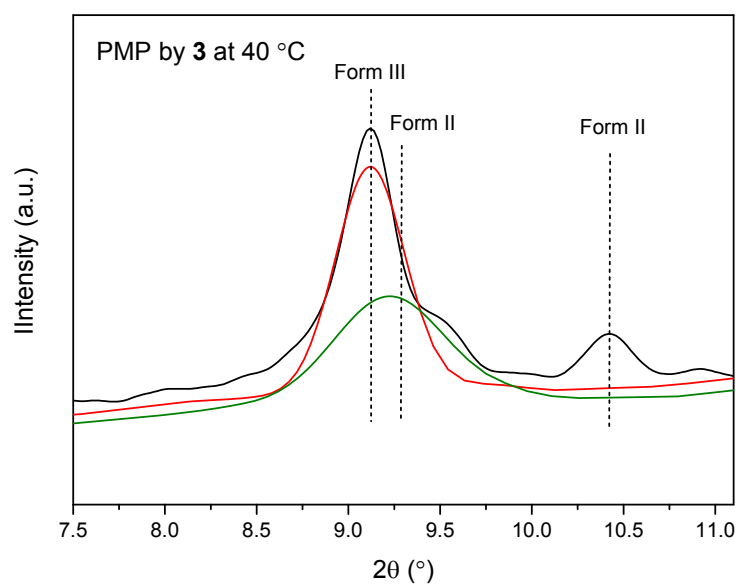


Figure S19. Peak separation of the X-ray diffraction patterns by **3** at 40 °C.

Table S1. Diffraction angles 2θ and Bragg spacings d of the reflections observed in the XRD patterns of the PMPs

Form I			Form II			Form III		
2θ ($^{\circ}$)	d (\AA)	(hkl)	2θ ($^{\circ}$)	d (\AA)	(hkl)	2θ ($^{\circ}$)	d (\AA)	(hkl)
9.48	9.32	200	9.26	9.54	100	9.08	9.73	200
13.44	6.58	220	10.44	8.47	020	12.92	6.85	220
16.70	5.30	212	10.96	8.07	$1\bar{2}0$	16.30	5.43	211
18.34	4.83	321	13.26	6.67	011	18.32	4.84	400
20.66	4.30	113, 411	15.00	5.90	$1\bar{1}1$	20.78	4.27	420, 321
21.66	4.10	322, 203	16.34	5.42	021, $1\bar{2}1$	22.74	3.91	411
			17.40	5.09	111, $2\bar{2}0$	26.36	3.38	431, 501
			18.56	4.78	200			
			19.70	4.50	031			
			20.44	4.34	040, 121			
			21.24	4.18	$2\bar{2}1$			
			22.78	3.90	$2\bar{3}1, 1\bar{4}1$			
			24.28	3.66	041			
			25.80	3.45	140, $1\bar{1}2$			

The data taken from references Macromolecules 1994, 27, 3864-3868; Macromolecules 2003, 36, 6087-6094; Polymer, 1987, 28, 1321; ACS Appl. Mater. Inter. 2011, 3, 969-977.

Table S2. Diffraction angles 2θ and Bragg spacings d of the reflections observed in the XRD patterns of the PMPs

Form IV			Form V		
2θ ($^\circ$)	d (\AA)	(hkl)	2θ ($^\circ$)	d (\AA)	(hkl)
8.05	10.98	110	8.54	10.35	
9.40	9.40	200	12.08	7.32	
12.10	7.31	210	15.29	5.79	
16.40	5.40	310	16.16	5.48	
18.20	4.87	211	17.10	5.18	
21.15	4.20	311	17.58	5.04	
24.50	3.63	401	18.43	4.81	
26.85	3.32	411	19.24	4.61	
28.35	3.15	511	19.49	4.55	
29.50	3.03	202, 212	21.34	4.16	
36.40	2.47	531, 701	25.00	3.56	
			28.13	3.17	

The data of Form IV taken from references Macromolecules 1999, 32, 935–938; ACS Appl. Mater. Inter. 2011, 3, 969–977. The data of Form V taken from references Macromolecules 1981, 14, 1390–1394; Polymer 1984, 25, 1619–1625.

References:

1. De Rosa, C.; Borriello, A.; Venditto, V.; Corradini, P. Crystal Structure of Form III and the Polymorphism of Isotactic Poly(4-methylpentene-1). *Macromolecules* **1994**, *27*, 3864–3868.
2. De Rosa, C. Crystal Structure of Form II of Isotactic Poly(4-methyl-1-pentene). *Macromolecules* **2003**, *36*, 6087–6094.
3. Charlet, G.; Delmas, G. Effect of solvent on the polymorphism of poly(4-methylpentene-1): 2. Crystallization in semi-dilute solutions. *Polymer*, **1987**, *28*, 1321.
4. Daniel, C.; Vitillo, J. G.; Fasano, G.; Guerra, G. Aerogels and Polymorphism of Isotactic Poly(4-methyl-pentene-1). *ACS Appl. Mater. Interfaces* **2011**, *3*, 969–977.
5. De Rosa, C. Chain Conformation of Form IV of Isotactic Poly(4-methyl-1-pentene). *Macromolecules* **1999**, *32*, 935–938.
6. Aharoni, S. M.; Charlet, G.; Delmas, G. Investigation of solutions and gels of poly(4-methyl-1-pentene) in cyclohexane and decalin by viscosimetry, calorimetry, and x-ray diffraction. A new crystalline form of poly(4-methyl-1-pentane) from gels. *Macromolecules* **1981**, *14*, 1390–1394.
7. Charlet, G.; Delmas, G. Effect of Solvent on the Polymorphism of Poly(4-methylpentene-1): 2. Crystallization in Semi-dilute Solutions. *Polymer* **1984**, *25*, 1619–1625.